Inorg. Chem. **1992**, *31*, 1050–1054

Contribution from the Department of Chemistry, Baker Laboratory,
Cornell University, Ithaca, New York 14853-1301

New Layered Ternary Niobium Tellurides: Synthesis, Structure, and Properties of $NbMTe_2$ (M = Fe, Co)

Jing Li,*,† Michael E. Badding, and F. J. DiSalvo

Received June 5, 1991

The layered ternary niobium tellurides $NbMTe_2$ (M = Fe, Co) have been synthesized by high-temperature solid-state reactions. The structures were determined by single-crystal X-ray diffraction methods, and both were found to be orthorhombic. $NbFeTe_2$ crystallizes in the space group *Pmna* (No. 53) with $Z = 4$, $a = 7.922$ (1) Å, $b = 7.239$ (1) Å, $c = 6.243$ (1) Å, $V = 357.98$ (9) Å^3, and $R = 4.11\%$, $R_w = 5.18\%$. $NbCoTe_2$ crystallizes in the space group *Cmca* (No. 64) with $Z = 8$, $a = 7.840$ (1) Å, $b = 14.431$ (2) Å, $c = 6.237$ (1) Å, $V = 705.7$ (2) Å^3, and $R = 2.92\%$, $R_w = 3.46\%$. The related $NbMTe_2$ compounds have a layered framework structure, consisting of a plane of distorted honeycombs of Nb (Nb–Nb = 3.187–3.213 Å), with pairs of M atoms (M–M = 2.488 Å in $NbFeTe_2$ and M–M = 2.499 Å in $NbCoTe_2$) sitting at the center of every Nb hexagon (one M above and one M below the Nb plane). The metal layers are capped above and below by tellurium atoms, leading to a tetrahedral coordination for M and a pseudooctahedral environment for Nb. The shortest interlayer Te–Te distance, 3.8 Å, is typical of van der Waals bonding between Te layers. Temperature-dependent conductivity and susceptibility measurements indicate metallic and Pauli-paramagnetic behavior of $NbCoTe_2$. $NbFeTe_2$ is metallic, and Fe has a low magnetic moment of 3.0 μ_B/Fe. The magnetic data suggest ferromagnetic intralayer interactions but antiferromagnetic interlayer interactions leading to a $T_N \approx 20$ K.

Introduction

Low dimensionality is a common feature of many niobium and tantalum chalcogenide compounds. Examples include binary phases MX_2 (M = Nb, Ta; X = S, Se, Te),[1] MX_3 (M = Nb, Ta; X = S, Se),[2] MTe_4 (M = Nb, Ta),[3] Nb_3X_4 (X = S, Se, Te),[4] and Ta_2X (X = S, Se)[5] and ternary phases $M_2Ta_9S_6$, $M_2Ta_{11}Se_8$ (M = Fe, Co, Ni),[6] $NbMTe_5$ (M = Ni, Pd),[7] $TaMTe_5$ (M = Ni, Pt),[8] $Ta_3Pd_3Te_{14}$,[8] and Ta_4MTe_4 (M = Si, Al, Cr, Fe, Co, Ni).[9] Interesting properties, such as superconductivity,[10] charge density waves,[11] and anisotropic electrical conductivity and optical behavior,[12] have been discovered in members of this family. Some of these compounds are also well-known for their important intercalation chemistry.[13] Band calculations have also revealed a number of interesting features in their electronic structures.[14]

Although numerous investigations have been conducted on binary niobium/tantalum chalcogenides, ternary compounds, especially tellurides, have received much less attention. For example, only some 10 ternary tantalum telluride phases have so far been reported in the literature, and their chemical and physical properties have not been well studied.

Encouraged by the discovery of the novel one-dimensional chain tantalum telluride compound Ta_4SiTe_4,[9] we have continued searching for more new ternary phases of low dimensionality. Here we report the synthesis, structure, and physical properties of the layered ternary niobium telluride compounds $NbMTe_2$ (M = Fe, Co).

Indeed, others have had a similar motivation. During the course of this work, we discovered several short papers by Huang et al. which report the synthesis and structure of $NbNiTe_2$ (*Pma*2), $TaNiTe_2$ (*Pma*2), and $NbCoTe_2$ ($P2_1/c$). We also received a preprint from Tremel on $NbCoTe_2$.[15] However, we find some differences in the structure and also here report for the first time the electrical and magnetic properties of this phase.

Sample Preparation

Nb (99.8%, Strem Chemicals, Newburyport, MA), Co (99.8%, Alfa Products, Ward Hill, MA), Fe (99.999%, Johnson Matthey Chemicals, Inc., London), and Te (99.999%, Alfa Products, Ward Hill, MA) were used as starting materials. $NbCoTe_2$ was first found in a reaction of a mixture of Nb, Co, and Te in a 4:5:10 molar ratio. The sample was sealed in an evacuated SiO_2 tube and heated to 800 °C for 3 days, followed by rapid quenching to room temperature. A small amount of tellurium tetrachloride ($TeCl_4$, ~10 mg) was used as a transport agent. Small platelike crystals were analyzed by microprobe (Superprobe 733). The result clearly indicated the presence of all three elements.

Attempts to grow larger crystals were made by varying the reaction conditions and the stoichiometric ratio of the reactants. Well-formed crystals of suitable size for single-crystal X-ray diffraction were obtained by reacting the elements Nb, Co, and Te (molar ratio 2:3:5, in the

---

* To whom correspondence should be addressed.

† Current address: Department of Chemistry, Rutgers University, Camden College of Arts and Sciences, Camden, NJ 08102.

(1) (a) Jellinek, F.; Brauer, G.; Müller, H. *Nature (London)* **1960**, *185*, 376. (b) Brown, B. E.; Beerntsen, D. J. *Acta Crystallogr.* **1965**, *18*, 31. Brixner, L. H. *J. Inorg. Nucl. Chem.* **1962**, *24*, 257. (c) Jellinek, F. *Ark. Kemi* **1963**, *20*, 447. Kadijk, F.; Huisman, R.; Jellinek, F. *Recl. Trav. Chim. Pays-Bas* **1964**, *83*, 768. Selte, K.; Bjerkelund, E.; Kjekshus, A. *J. Less-Common Met.* **1966**, *11*, 14.

(2) Sambong, T.; Tsutsumi, K.; Shiozaki, K.; Yamamoto, M.; Yamaya, K.; Abe, Y. *Solid State Commun.* **1977**, *22*, 729. Rijnsdorp, J.; Jellinek, F. *J. Solid State Chem.* **1978**, *25*, 325. Hodeau, J. L.; Marezio, M.; Roncau, C.; Ayroles, R.; Meerschaut, A.; Rouxel, J.; Monceau, P. *J. Phys. C* **1978**, *11*, 4117. Bjerkelund, E.; Fermor, J. H.; Kjekshus, A. *Acta Chem. Scand.* **1966**, *20*, 1836.

(3) Bjerkelund, E.; Kjekshus, A. *J. Less-Common Met.* **1964**, *7*, 231. Selte, K.; Kjekshus, A. *Acta Chem. Scand.* **1964**, *18*, 690.

(4) Selte, K.; Kjekshus, A. *Acta Crystallogr.* **1964**, *17*, 1568. Ruysink, A. F. J.; Kadijk, F.; Wagner, A. J.; Jellinek, F. *Acta Crystallogr., Sect. B* **1968**, *24*, 1614.

(5) Franzen, H. F.; Smeggil, J. G. *Acta Crystallogr., Sect. B* **1969**, *25*, 1736. Harbrecht, B. *Angew. Chem., Int. Ed. Engl.* **1989**, 1660.

(6) Harbrecht, B.; Frazen, H. F. *J. Less-Common Met.* **1986**, *115*, 177. Harbrecht, B. *Ibid.* **1986**, *124*, 125; **1988**, *141*, 59.

(7) Liimatta, E. W.; Ibers, J. A. *J. Solid State Chem.* **1987**, *71*, 384; **1988**, *77*, 141.

(8) Liimatta, E. W.; Ibers, J. A. *J. Solid State Chem.* **1989**, *78*, 7.

(9) Badding, M. E.; DiSalvo, F. J. *Inorg. Chem.* **1990**, *29*, 3953.

(10) (a) Amberger, E.; Polborn, K.; Grimm, P.; Dietrich, M.; Obst, B. *Solid State Commun.* **1978**, *26*, 943. (b) Biberacher, W.; Schwenk, H. *Solid State Commun.* **1980**, *33*, 385. (c) Ishihara, Y.; Nakada, I. *Solid State Commun.* **1982**, *42*, 579. (d) *Ternary Superconductors*; Shenoy, G. K., Dunlap, B. D., Fradin, F. Y., Eds.; Elsevier North Holland, Inc.: New York, 1981.

(11) (a) Wilson, J. A.; DiSalvo, F. J.; Mahajan, S. *Adv. Phys.* **1975**, *24*, 117. (b) Ishihara, Y.; Nakada, I. *Solid State Commun.* **1983**, *45*, 129. (c) Nakada, I.; Suzuki, K.; Ichihara, M. *Solid State Commun.* **1984**, *50*, 657. (d) Suzuki, K.; Ichihara, M.; Nakada, I.; Ishikara, Y. *Solid State Commun.* **1984**, *52*, 743; **1986**, *59*, 291. (e) *Electronic Properties of Inorganic Quasi One-Dimensional Compounds*; Monceau, P., Ed.; Reidel: Dordrecht, The Netherlands, 1985; Part 1–2. (f) *Crystal Chemistry and Properties of Materials with Quasi One-Dimensional Structures*; Rouxel, P., Ed.; Reidel: Dordrecht, The Netherlands, 1986.

(12) Wilson, J. A.; Yoffe, A. D. *Adv. Phys.* **1969**, *18*, 193. See also refs 10a,b and 11a,b.

(13) Schollhorn, R.; Schramm, W. *Z. Naturforsch., B* **1979**, *34*, 697. Schollhorn, R.; Schramm, W.; Fenske, D. *Angew. Chem., Int. Ed. Engl.* **1980**, *19*, 492. Boller, H.; Klepp, K. *Mater. Res. Bull.* **1983**, *18*, 437. Huan, G.; Greenblatt, M. *Mater. Res. Bull.* **1987**, *22*, 505, 943.

(14) Oshiyama, A. *Solid State Commun.* **1982**, *8*, 607. Oshiyama, A. *J. Phys. Soc. Jpn.* **1983**, *52*, 587. Canadell, E.; Whangbo, M.-H. *Inorg. Chem.* **1986**, *25*, 1488. Bullett, D. W. *J. Solid State Chem.* **1980**, *33*, 13. Calhorda, M. J.; Hoffmann, R. *Inorg. Chem.* **1988**, *27*, 4679. Halet, J.-F.; Hoffmann, R.; Tremel, W.; Liimatta, E. W.; Ibers, J. A. *Chem. Mater.* **1989**, *1*, 451. Li, J.; Hoffmann, R.; Badding, M. E.; DiSalvo, F. J. *Inorg. Chem.* **1990**, *29*, 3943.

(15) $NbCoTe_2$: Huang, B.; Shang, B.; Huang, J. *Jiegou Huaxue* **1988**, *7*, 133. Tremel, W. Manuscript submitted to *J. Chem. Soc., Chem. Commun.* $NbNiTe_2$: Huang, B.; Shang, B.; Huang, J. *Jiegou Huaxue* **1988**, *7*, 214. $TaNiTe_2$: Huang, B.; Shang, B.; Huang, J. *Jiegou Huaxue* **1989**, *8*, 145.

0020-1669/92/1331-1050$03.00/0

Table I. Crystallographic Data for $NbCoTe_2$

chem formula $NbCoTe_2$	fw 407.0
$a = 7.8400$ (10) Å	space group *Cmca* (No. 64)
$b = 14.431$ (2) Å	$T = 25$ °C
$c = 6.2370$ (10) Å	$\lambda = 0.71073$ Å
$\alpha = \beta = \gamma = 90°$	$\rho_{calcd} = 7.662$ g cm^{-3}
$V = 705.7$ (2) Å^3	$R^a = 2.92\%$
$Z = 8$	$R_w{}^b = 3.46\%$

$^a R = \sum(|F_o| - |F_c|)/\sum(|F_o|)$. $^b R_w = [\sum(w(|F_o| - |F_c|)^2)/\sum(w|F_o|^2)]^{1/2}$, $w = 1/(\sigma^2(F_o) + 0.0001F_o^2)$.

Table II. Crystallographic Data for $NbFeTe_2$

chem formula $NbFeTe_2$	fw 404.0
$a = 7.9220$ (10) Å	space group *Pmna* (No. 53)
$b = 7.2390$ (10) Å	$T = 25$ °C
$c = 6.2430$ (10) Å	$\lambda = 0.71073$ Å
$\alpha = \beta = \gamma = 90°$	$\rho_{calcd} = 7.495$ g cm^{-3}
$V = 357.98$ (9) Å^3	$R^a = 4.11\%$
$Z = 4$	$R_w{}^b = 5.18\%$

$^a R = \sum(|F_o| - |F_c|)/\sum(|F_o|)$. $^b R_w = [\sum(w(|F_o| - |F_c|)^2)/\sum(w|F_o|^2)]^{1/2}$, $w = 1/(\sigma^2(F_o) + 0.0001F_o^2)$.

Table III. Atomic (Fractional) Coordinates and Equivalent Isotropic Displacement Coefficients (Å^2 × 10^3)

atom	site	*x*	*y*	*z*	*U*(eq)^a
			$NbCoTe_2$		
Nb	8d	0.2968 (1)	0.5	0.0	17 (1)
Co	8f	0.0	0.4413 (1)	0.1473 (1)	15 (1)
Te1	8e	0.25	0.3393 (1)	0.25	16 (1)
Te2	8f	0.5	0.6127 (1)	0.2518 (1)	18 (1)
			$NbFeTe_2$		
Nb	4f	0.7981 (1)	0.5	0.0	22 (1)
Fe	4h	0.0	0.3836 (3)	0.6465 (2)	20 (1)
Te1	4g	0.75	0.1808 (1)	0.75	18 (1)
Te2	4h	0.0	0.7257 (1)	0.7508 (1)	25 (1)

^{a} Equivalent isotropic *U* defined as one-third of the trace of the orthogonalized U_{ij} tensor.

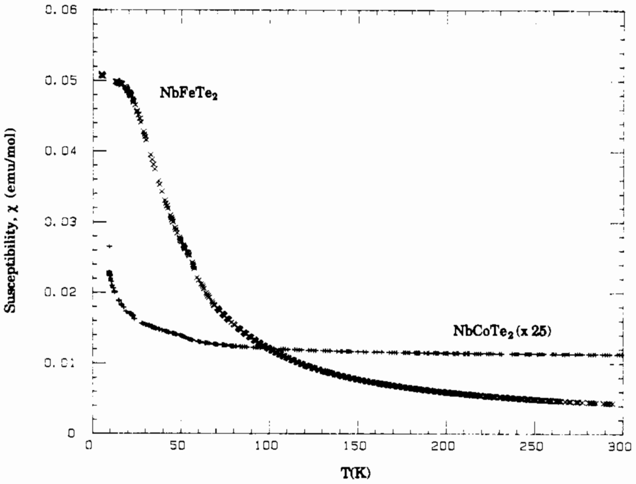

Figure 1. Temperature dependence of the susceptibility of $NbFeTe_2$ and $NbCoTe_2$ (4–300 K).

presence of $TeCl_4$) in an evacuated and sealed quartz tube at 925 °C for 2 days.

The same heating scheme was used to obtain a polycrystalline sample of $NbCoTe_2$ starting from a stoichiometric mixture of the three elements. The X-ray powder diffraction pattern of this sample, taken on a Scintag 2000 powder diffractometer, is consistent with the calculated pattern from the single-crystal data.

Appropriate crystals of $NbFeTe_2$ were also obtained by reacting the elements, Nb, Fe, and Te, in the molar ratio of 2:3:5. The mixture was sealed in an evacuated quartz tube, which was placed in a furnace and heated to 850 °C for 5 days. Approximately 10 mg of $TeCl_4$ was included as a transport agent. After the reaction, the container was cooled by quenching to room temperature.

Our attempts to obtain a stoichiometric polycrystalline sample of $NbFeTe_2$ were not successful. Samples prepared below 900 °C always contained a ferromagnetic impurity phase, probably a small amount of unreacted Fe. Samples prepared above 900 °C no longer contain that ferromagnetic phase, but the powder patterns will show a few weak impurity lines. Above 1100 °C, the compound begins to melt incongruently.

Crystals of both $NbFeTe_2$ and $NbCoTe_2$ show metallic luster and are air stable. A simple "tape-test" clearly indicates their layerlike nature.[16]

Structure Determination

Structure determination of $NbCoTe_2$ was performed on a 0.20 × 0.17 × 0.02 mm^3 single crystal. Rotational and axial photographs revealed Laue symmetry (*mmm*) and yielded approximate lattice parameters. Final unit cell constants were obtained with a least-squares analysis of 26 reflections selected from a shell data collection ($2\theta = 15$–$23°$). Data were collected on a Syntex $P2_1$ diffractometer using Mo Kα radiation and a graphite monochromator. Three diffraction peaks (check reflections) were remeasured after each set of 50 reflections; these monitored the process and their consistency indicated no decomposition during the data collection. Four octants of data were collected and merged to improve the solution. Systematic absences reduced the possible space groups to the *C*-centered orthorhombic *Cmca* (No. 64) and *C2cb* (No. 41). The final structure was solved by direct methods in the centrosymmetric space group *Cmca*. The structure solution and refinement were carried out using SHELXTL Plus[17] running on a Microvax computer. An analytical absorption correction procedure was employed at an early stage of the refinement. The largest peak and largest hole in the final difference Fourier map were 1.83 and −1.60 e Å^{-3}, respectively. Final refinement generated $R = 2.92\%$ and $R_w = 3.46\%$. The atomic positions and refined *R* factors in the noncentrosymmetric space group *C2cb* were not significantly different from those in *Cmca*. The analytical forms of the scattering factor tables for the neutral atoms were used[18] and all scattering factors were corrected for both real and imaginary components of anomalous dispersion.[19] Table I lists some crystal data and parameters for the data collection and refinement process.

The same procedure was used to determine the structure of $NbFeTe_2$. A crystal 0.14 × 0.12 × 0.02 mm^3 was selected for the data collection. The Laue symmetry was found again to be *mmm*. The final lattice parameters were obtained from 28 reflections collected in a shell ($15° < 2\theta < 23°$). Four octants of data were collected and merged. An analytical absorption correction was performed. Systematic absences narrowed the possible space groups to *Pmna* (No. 53) and *Pnc*2 (No. 30). The structure was solved by direct methods and refined in the centrosymmetric space group *Pmna*. Final $R = 4.11\%$ and $R_w = 5.18\%$ were obtained. Table II summarizes the crystal data and parameters for the data collection and refinement process. The fractional atomic coordinates and thermal parameters for both structures are tabulated in Table III.

Magnetic Susceptibility Measurement

The temperature-dependent magnetic susceptibilities of both compounds were measured with a Faraday balance.[20] The measurements were performed on a powder sample of $NbCoTe_2$ (100 mg) and a powder sample prepared from single crystals of $NbFeTe_2$ (17 mg, ground). The room-temperature susceptibility of the $NbCoTe_2$ was found to be field independent, whereas an Owens and Honda plot[21] for $NbFeTe_2$ at room temperature showed a small field dependence, indicating the presence of a small amount of a ferromagnetic impurity phase. Such ferromagnetic contamination was probably due to unreacted Fe (~1 μg, 0.04% Fe in the sample) and was subtracted from the data using the method by Owen and Honda.[21]

---

(16) Tape-test: A platelike crystal was placed onto a piece of Scotch Brand tape. The tape was then folded over onto the crystal. Upon opening of the tape, the crystal was cleaved into two parts (identical in shape, but thinner). The process was repeated until the crystals became so thin that they appeared transparent to the eye.

(17) Release of 3.4 of SHELXTL Plus for Nicolet Crystallographic Research Systems.

(18) Cromer, D. T.; Waber, J. T. *International Tables for X-Ray Crystallography*; Kynoch Press: Birmingham, England, 1974; Vol. IV, Table 2.2B.

(19) Cromer, D. T.; Waber, J. T. *International Tables for X-Ray Crystallography*; Kynoch Press: Birmingham, England, 1974; Vol. IV, Table 2.3.1.

(20) Vassiliou, J. K.; Hornbostel, M.; Ziebarth, R.; DiSalvo, F. J. *J. Solid State Chem.* **1989**, *81*, 208.

(21) Selwood, P. W. *Magnetochemistry*; Wiley-Interscience: New York, 1989; p 186.

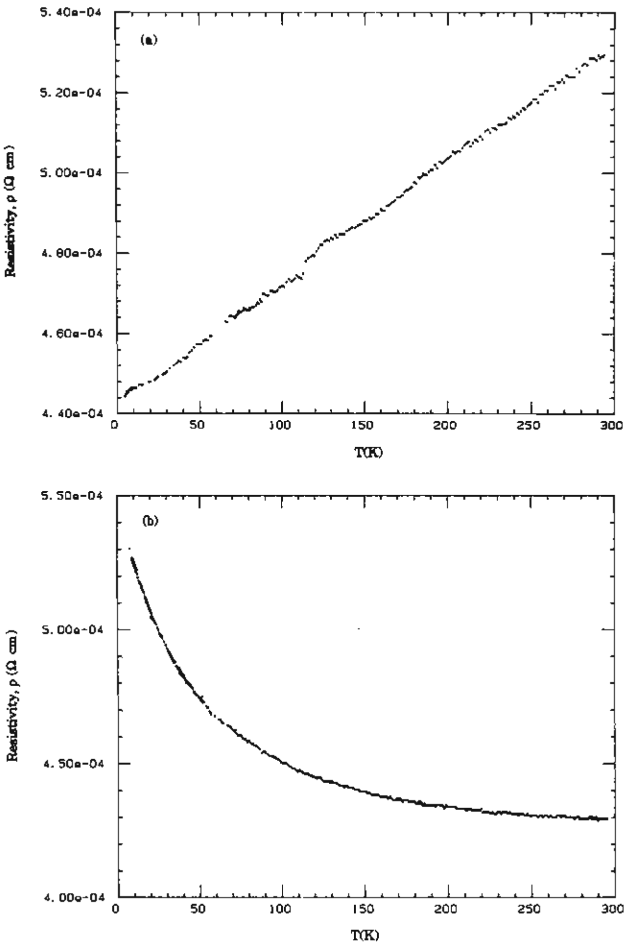

Figure 2. Temperature dependence of the resistivity of $NbMTe_2$: (a) ρ–T curve for $NbCoTe_2$; (b) ρ–T curve for $NbFeTe_2$.

The susceptibility versus temperature curves for both samples are plotted in Figure 1 from 4 to 300 K. Both curves were fit to the Curie–Weiss form by a least-squares procedure:

$$\chi = \chi_0 + C/(T + \Theta)$$

where χ_0 is the temperature-independent contribution to the total susceptibility and C and Θ are the Curie and Weiss constants, respectively. This expression is expected to describe the susceptibility of most materials when $T > \Theta$ (often T must be greater than Θ by several factors). For $NbCoTe_2$, a fit over the temperature interval of $6\ K < T < 300\ K$ gave $\chi_0 = (4.25 \pm 0.08) \times 10^{-4}$ emu/mol, $C = (6.4 \pm 0.8) \times 10^{-3}$ emu K/mol, and $\Theta = 3 \pm 2$ K, with a mean square deviation of 1.41%. For $NbFeTe_2$, a fit over $40\ K < T < 300\ K$ gave $\chi_0 = (6.8 \pm 0.2) \times 10^{-4}$ emu/mol, $C = 1.08 \pm 0.08$ emu K/mol, and $\Theta = -10 \pm 3$ K, with a mean square deviation of 1.33%. The three parameters in this fit are correlated. The precession quoted for each is determined by the values at which the mean square deviation increases by 0.2%. Note for both samples a small anomaly in χ near 50 K indicates the presence of a small amount of paramagnetic O_2 that solidified on the sample during the susceptibility measurements.

Electrical Conductivity Measurement

Samples used for the conductivity measurement were in the form of a pellet (sintered at 950 °C, 0.5 in. in diameter, 0.047 in. in thickness) of $NbCoTe_2$ and a single crystal ($0.95 \times 0.86 \times 0.079$ mm^3) of $NbFeTe_2$. The resistance was measured using the four-probe method at 40 Hz by lock-in detection. In the case of $NbCoTe_2$, contacts were made by pressing the four spring-loaded and gold-plated pins, arranged collinearily, against the flat surface of the pellet. Ohmic behavior was apparent from the linearity of the I–V characteristics (~10–70 mA). The system was calibrated by measuring the resistance of a solid molybdenum disk (0.5 in. in diameter and 0.068 in. in thickness). A proportionality constant relating the sample resistance to the resistivity was thus obtained.[22] This value was used to convert the measured resistance of the sample to its resistivity. The resulting temperature-dependent resistivity of $NbCoTe_2$ between 4 and 300 K is shown in Figure 2a (the somewhat noisy behavior between 115 and 135 K was due to a slight shift of voltage contacts as the system contracted on cooling). In the case of $NbFeTe_2$, the resistivity in the a–c plane was determined using van der Pauw's technique.[23] Four indium contacts were made to the crystal with an ultrasonic soldering iron. The crystal was then placed onto a piece of sapphire, and gold wires were attached to the contacts with silver paste. Figure 2b shows the resistivity of $NbFeTe_2$ in the temperature range 4–300 K.

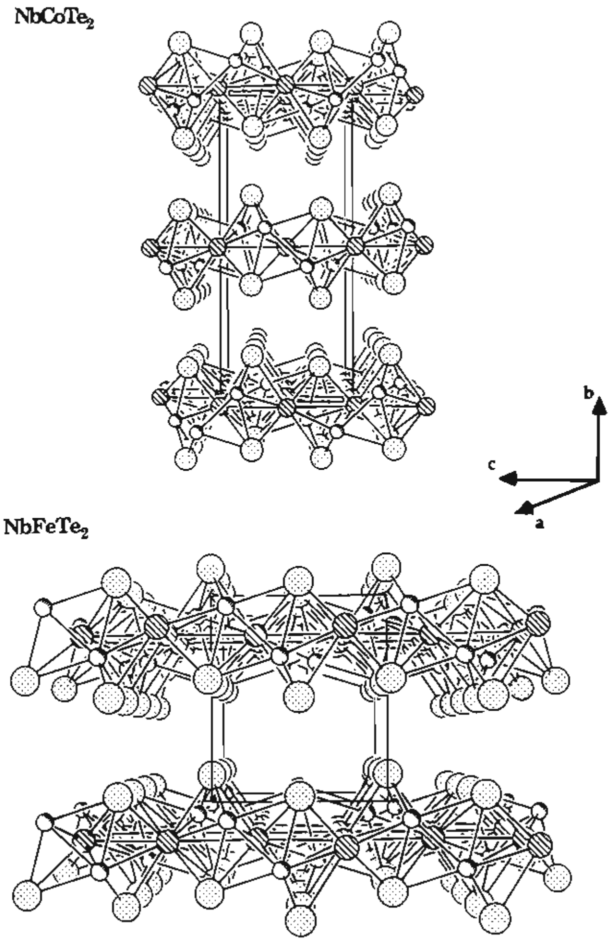

Figure 3. Perspective views of the layered $NbMTe_2$ (M = Fe, Co) structure. The shortest Te–Te interlayer distances are ~3.8 Å in both structures. The hatched circles are the Nb atoms; partially hatched circles, M atoms; and dotted circles, Te atoms.

Results and Discussion

Both $NbFeTe_2$ and $NbCoTe_2$ crystallize in a layered structure type. As shown in Figure 3, each layer consists of a central sheet of Nb atoms bonded to M (Fe or Co) pairs, which are sandwiched above and below by Te atoms. The only difference between the two structures, which is reflected in the fact that $NbCoTe_2$ has a C-centered unit cell while $NbFeTe_2$ has a primitive unit cell, is a different sequence of stacking the "sandwiches" along the b axis; the $NbCoTe_2$ sandwiches stack with the Co–Co dumbbells shifted by $^1/_2$ translation along a, whereas the $NbFeTe_2$ sandwiches stack with the Fe–Fe dumbbells directly above each other. The intralayer atomic distances are short, representing typical covalent bond lengths; the interlayer contacts are however large, characteristic of van der Waals interactions. Within a layer, Nb atoms form a distorted honeycomb net in the a–c plane. The average Nb–Nb distance is quite long, ~3.2 Å. At the center of every honeycomb lies a pair of M atoms, one above and one below the Nb plane. The M–M distances, Fe–Fe = 2.488 Å and Co–Co = 2.499 Å, are comparable to those found in their corresponding metals (2.482 and 2.506 Å, respectively).[24] Each

---

(22) Wasscher, J. D. *Philips Res. Rept.* **1961**, *16*, 301.

(23) van der Pauw, L. J. *Philips Res. Rept.* **1958**, *13*, 1.

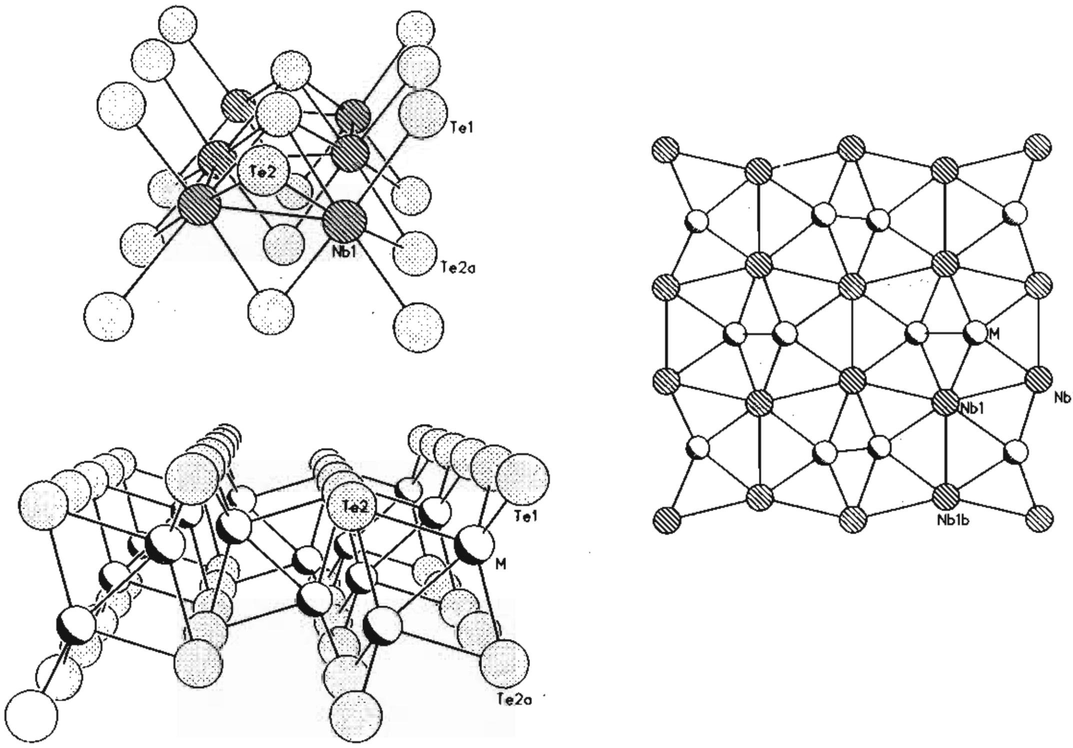

Figure 4. Coordination environment of the atoms in $NbMTe_2$. The hatched circles are the Nb atoms; partially hatched circles, M atoms; and dotted circles, Te atoms.

Table IV. Important Interatomic Distances (Å)

	(a) $NbCoTe_2$		
Co1–Nb1	2 × 2.641 (1)	Nb1–Nb1a	2 × 3.204 (1)
Co1–Nb1a	2 × 2.845 (1)	Nb1–Nb1b	3.187 (1)
	Co1–Co1a	2.499 (2)	
Co1–Te1	2 × 2.534 (1)	Nb1–Te1	2 × 2.819 (1)
Co1–Te2	2.587 (1)	Nb1–Te2	2 × 2.766 (1)
Co1–Te2a	2.552 (1)	Nb1–Te2a	2 × 3.234 (1)
	(b) $NbFeTe_2$		
Fe1–Nb1	2 × 2.669 (1)	Nb1–Nb1a	2 × 3.213 (1)
Fe1–Nb1a	2 × 2.853 (1)	Nb1–Nb1b	3.199 (2)
	Fe1–Fe1a	2.488 (3)	
Fe1–Te1	2 × 2.548 (1)	Nb1–Te1	2 × 2.814 (1)
Fe1–Te2	2.604 (2)	Nb1–Te2	2 × 2.765 (1)
Fe1–Te2a	2.561 (2)	Nb1–Te2a	2 × 3.271 (1)

niobium atom is bonded to four M atoms and, at longer distances, to three Nb atoms, while each M atom is bonded to another M and four Nb atoms. The coordination environments of Nb and M are displayed in Figure 4. The metal-to-tellurium coordination can be described as distorted tetrahedral for M (cobalt 2 × 2.534, 2.552, 2.587 Å; iron 2 × 2.548, 2.561, 2.604 Å) and pseudooctahedral for niobium with four short bonds ($NbCoTe_2$ 2 × 2.766, 2 × 2.819 Å; $NbFeTe_2$ 2 × 2.765, 2 × 2.814 Å) and two long bonds ($NbCoTe_2$ 2 × 3.234 Å; $NbFeTe_2$ 2 × 3.271 Å). Note that the two long Nb–Te distances are cis to each other. Pertinent interatomic distances for both structures are listed in Table IV.

Many layered transition metal telluride structures contain close-packed or sections of close-packed tellurium sublattices. Two kinds of interstices are found in these close-packed layers: T (tetrahedral, T^+ and T^-) sites and O (octahedral) sites, which are often partially occupied by transition metal elements. In our $NbMTe_2$ structure, the close-packed tellurium layers are very distorted from ideal geometry. Half of the distorted tetrahedral sites are filled by M atoms which form pairs by occupying adjacent sites. To allow such pairing, the tellurium layers are distorted by shifting one layer with respect to the other in the direction parallel to the M–M bond, as well as slightly puckering along the packing axis. The distortion also shifts the niobium atoms, which fill the distorted octahedral sites, so that every two adjacent Nb atoms form a weak bond across the empty distorted tetrahedral sites (reduced in size) to make more room for the other half of the T sites to fit the M pair.

The occurrence of a pair of bonded cationic atoms surrounded by polyhedral anions is not very common in solids. In chalcogenide compounds containing other main group elements, the MPX_3 (M = Mn, Fe, Co, Ni, Cd; X = S, Se) layered phases are one example of this behavior, where the phosphorus forms P_2 pairs at the center of a distorted S_6 octahedron.[25] Si_2Te_3,[26] $K_6Si_2Te_6$,[27] $Mn_3Si_2Te_6$,[28] and $Cr_2Si_2Te_6$[29] are the only known silicon telluride phases containing Si_2 pairs. Pairing is also found in some Ge chalcogenide structures, $Na_8Ge_4Se_{10}$,[30] $Na_6Ge_2Se_{16}$,[30] and $K_6Ge_2Te_6$.[31] As far as we know, there is no report of transition metal chalcogenide compounds with pairs of transition metal atoms in a similar coordination environment, except in the recent work of Huang et al. and Tremel.[15]

According to their reports, the structure of $NbCoTe_2$, synthesized at a higher temperature (1000 °C), is monoclinic (space group $P2_1/c$ with a = 8.197 Å, b = 6.258 Å, c = 7.816 Å, β = 118.48°). Their final R, R_w were 6.2%, 7.9% (Huang) and 5.9%, 6.0% (Tremel). Our single-crystal data, however, clearly show a higher symmetry C-centered orthorhombic cell for this structure. In fact, applying a standard search for higher symmetry to the reported monoclinic cell parameters gives a C-centered orthorhombic cell nearly identical to the cell we report. The powder X-ray diffraction patterns generated by LAZY[32] were almost

---

(24) *Tables of Interatomic Distances and Configurations in Molecules and Ions, Supplement, 1956–1959*; Sutton, L. E., et al., Eds.; Special Publication No. 18; The Chemical Society: London, 1965.

(25) Hahn, H.; Klingen, W. *Naturwissenschaften* **1965**, *52*, 494. Klingen, W.; Eulenberger, G.; Hahn, H. *Z. Anorg. Allg. Chem.* **1973**, *401*, 97. Ouvrard, G.; Brec, R.; Rouxel, J. *Mater. Res. Bull.* **1985**, *20*, 1181. Brec, R. *Solid State Ionics* **1986**, *22*, 3.

(26) Ploog, K.; Stetter, W.; Nowitzki, A.; Schönherr, E. *Mater. Res. Bull.* **1976**, *11*, 1147.

(27) Dittmar, G. *Acta Crystallogr., Sect. B* **1978**, *34*, 2390.

(28) Vincent, H.; Leroux, D.; Bijaoui, D.; Rimet, R.; Schlenker, C. *J. Solid State Chem.* **1986**, *63*, 349.

(29) Ouvrard, G.; Sandre, E.; Brec, R. *J. Solid State Chem.* **1988**, *73*, 27.

(30) Eisenmann, B.; Hansa, J.; Schäfer, H. *Mater. Res. Bull.* **1985**, *20*, 1339.

(31) Dittmar, G. *Z. Anorg. Allg. Chem.* **1978**, *453*, 68.

identical for the two sets of structural data (*Cmca* and $P2_1/c$), indicating perhaps how the structure could have been mistaken for monoclinic. Our final residues, $R = 2.92\%$ and $R_w = 3.46\%$, suggest an excellent refinement. On the basis of the above arguments, it is clear that the *Cmca* space group is correct for this structure.

The magnetic behavior of $NbCoTe_2$ (Figure 1) is typical of that for a metallic compound with a small paramagnetic impurity that leads to a Curie-like increase in susceptibility at low temperatures. The most likely impurity is Fe (assuming $\mu_{eff} = 5\ \mu_B$, we calculate ~530 ppm of Fe, which is consistent with the 99.8% purity of the Co used in preparing the sample). Thus, the Co atoms have no local magnetic moment. The χ_0 is positive ($\chi_0 = 4.25 \times 10^{-4}$ emu/mol), suggesting Pauli paramagnetism due to conduction electrons;[33-35] the metallic conductivity (see later discussion) makes this certain.

The magnetic properties of $NbFeTe_2$, on the other hand, are quite different from those of $NbCoTe_2$. The susceptibility of this material shows a strong temperature dependence. The calculated effective magnetic moment, $3.0 \pm 0.1\ \mu_B$/Fe or $4.2 \pm 0.1\ \mu_B$/Fe pair (~2 spins per Fe), indicates the formation of a local magnetic moment on Fe. The negative Θ ($\Theta = -10$ K) is characteristic of net ferromagnetic interactions. The fact that a saturation (or "turning over") of susceptibility was observed at ~20 K in the χ–T curve (Figure 1) may be explained if intralayer Fe–Fe interactions are assumed to be stronger and ferromagnetic and interlayer interactions are assumed to be weaker and antiferromagnetic. Intralayer interactions are assumed to be stronger because of the shorter Fe–Fe distances of 2.488 and 4.721 Å, while the shortest interlayer Fe–Fe distance is 5.849 Å. At high temperatures, the ferromagnetic contributions dominate the susceptibility. The antiferromagnetic interactions cause the magnetic susceptibility curve to turn over at ~20 K.[36] It is possible that the localized electron spins are formed from some narrow Fe 3d bands, and we hope to understand this with band calculations, which are in progress.[37] Note however that the Fe moment is considerably below 4.9 μ_B, a value expected for high-spin Fe^{2+}, perhaps indicating a possible lower oxidation state of Fe. An oxidation state of Fe^{3+} is very unlikely in a telluride; furthermore, that will leave the very electropositive Nb at a low oxidation state of +1.

The temperature-dependent electrical resistivity of $NbCoTe_2$ is linear with a positive slope (Figure 2a). The general features of the measured resistivity resemble those of many intermetallic compounds containing transition metals. The small change in its magnitude over the entire temperature range is consistent with the behavior of a poor metal with moderately large scattering. Notice that the curve does not become temperature independent at low T (<50 K), as is found in most other metallic compounds. The resistivity of $NbFeTe_2$, plotted in Figure 2b, exhibits a different temperature dependence: it increases slightly as temperature decreases. This unusual behavior may be due to strong coupling between the magnetic and conduction electrons.

Conclusion

We have synthesized and determined crystal structures of two ternary niobium tellurides, $NbMTe_2$ (M = Fe, Co). Both compounds crystallize in a layered structure type. Both are metallic. While the temperature-dependent conductivity of $NbCoTe_2$ is typical of that for a metal, it reveals some unusual features for $NbFeTe_2$. $NbCoTe_2$ exhibits Pauli-paramagnetic behavior, whereas the magnetic susceptibility data of $NbFeTe_2$ indicate local moment formation on Fe. The magnetic properties suggest ferromagnetic intralayer interactions and antiferromagnetic interlayer interactions.

Acknowledgment. We are grateful to the Department of Energy, Division of Basic Energy Sciences, for its generous support through Grant DE-FG02-87ER45298. We thank Greg VanDuyne (Chemistry Department Single Crystal X-ray Facility, Cornell University) for aid with the structure determinations.

Supplementary Material Available: Tables of structure determination summaries, atomic coordinates, thermal parameters, bond lengths, and bond angles (12 pages); listings of calculated and observed structure factors (4 pages). Ordering information is given on any current masthead page.

---

(32) A program to calculate theoretical X-ray and neutron diffraction powder patterns, written by C. Yvon, W. Jeitschko, and E. Parthé. For supplementary descriptions, see: *J. Appl. Crystallogr.* **1977**, *10*, 73.

(33) Kittel, C. *Introduction to Solid State Physics*, 6th ed.; Wiley: New York, 1986.

(34) Ashcroft, N. W.; Mermin, N. D. *Solid State Physics*; Saunders: Philadelphia, PA, 1976.

(35) Vandenberg-Voorhoeve, J. M. In *Optical and Electrical Properties*; Lee, P. A., Ed.; Physics and Chemistry of Materials with Layered Structures, Vol. 4; Reidel: Dordrecht, The Netherlands, 1976; p 423.

(36) Smart, J. S. *Effective Field Theories of Magnetism*; Saunders: Philadephia, London, 1966.

(37) Li, J. Manuscript in preparation.